



*J. Serb. Chem. Soc.* 88 (9) 905–919 (2023)  
JSCS–5670

## Mass transfer in inverse fluidized beds

DARKO JAĆIMOVSKI<sup>1</sup>, KATARINA ŠUĆUROVIĆ<sup>1#</sup>, MIHAL ĐURIŠ<sup>1#\*</sup>, ZORANA ARSENIJEVIĆ<sup>1#</sup>, SANJA KRSTIĆ<sup>2</sup> and NEVENKA BOŠKOVIĆ-VRAGOLOVIĆ<sup>3#</sup>

<sup>1</sup>*Institute of Chemistry, Technology and Metallurgy-National Institute of the Republic of Serbia, University of Belgrade, Belgrade, Serbia,* <sup>2</sup>*Vinča institute of Nuclear Sciences-National Institute of the Republic of Serbia, University of Belgrade, Belgrade, Serbia and* <sup>3</sup>*Faculty of Technology and Metallurgy, University of Belgrade, Belgrade, Serbia*

(Received 16 January, revised 27 February, accepted 22 March 2023)

**Abstract:** In this work, the coefficient of fluid-wall mass transfer in an inverse fluidized bed was determined using the adsorption method. The experiments were carried out in a column with a diameter of 45 mm with spherical and non-spherical particles of polypropylene and polyethylene with a diameter of 3.3–4.9 mm and a density of about 930 kg m<sup>-3</sup>. A diluted solution of methylene blue was used as a fluidization medium, which was adsorbed on part of the surface of the column on silica gel. The obtained results showed that the presence of particles during inverse fluidization does not contribute significantly to mass transfer compared to the influence of particles on transfer in conventional fluidized beds. Therefore, the pseudo-fluid concept was introduced into the analysis and an empirical correlation was performed to determine the mass transfer coefficient. The obtained results were compared with literature correlations for inverse and conventional fluidized beds.

**Keywords:** inverse fluidization; fluid-wall mass transfer; pseudo-fluid.

### INTRODUCTION

Fluidized bed contactors, because of their efficiency and transfer intensity, are often used in systems where contact between liquids and solid particles is required. When the solid phase has a lower density than the liquid phase, fluidization can be achieved by the liquid flowing into the column from the top and forming the bed in the opposite way compared to a conventional bed. Such beds are inverse fluidized beds.

Inverse fluidization is most commonly used in wastewater treatment in bio-reactors or in some adsorption processes. The beds formed this way have been

\* Corresponding author. E-mail: mihal.djuris@ihtm.bg.ac.rs

# Serbian Chemical Society member.

<https://doi.org/10.2298/JSC230116016J>

shown to be effective for formation and maintenance of biofilm. For the practical application of inverse fluidized beds in various contactors, it is necessary to know the fluid dynamics of these systems and the mass transfer achieved.

Wang *et al.*<sup>1</sup> studied the removal of oil from an emulsion in water by inverse fluidization with a hydrophobic air gel. The authors used nanogel sizes: 0.5–0.85 mm; 0.7–1.2 mm; 1.7–2.35 mm, the density was  $64 \text{ kg m}^{-3}$ . The experiments were performed in columns with a diameter of 7.6 cm and lengths of 1.47 m and 0.77 m. The oil concentration is monitored using the *COD* (chemical oxygen demand). The authors have proposed a model that is consistent with the experimental data. It has been shown that the most important parameters affecting oil removal and thus mass transfer are granule size, bed height and fluid velocity.

Inverse fluidization is applied in bioreactors where the necessary oxygen is supplied to the microorganisms in a three-phase fluidized bed. The application of inverse fluidization in fluidized bed biofilm reactors (FBBR) is shown in the work of Begum and Radha<sup>2</sup> in which the aerobic biodegradation of phenol was studied using the microorganism *Pseudomonas fluorescens*. The authors performed the experimental tests in a column with a height of 105 cm and a diameter of 10 cm. Polystyrene particles with a diameter of 3.5 mm and a density of  $863 \text{ kg m}^{-3}$  were used as biofilm carriers. Mass transfer is monitored by the parameter *COD*. It was shown that the value of *COD* removal increases with the gas velocity and the ratio of the volume of settled bed to the working volume ( $V_b/V_R$ ). In the best case, *COD* reduction is 98.5 %. Similarly, the biological treatment of wastewater in an inverse fluidized bed system was performed by Sokol *et al.*<sup>3</sup> These authors performed the removal of phenol, cresol, isopropylphenol, dimethylphenol, benzene and toluene from wastewater in a column with an internal diameter of 20 cm and a height of 6 m with polypropylene particles of density  $910 \text{ kg m}^{-3}$  as biofilm carriers in an inverse fluidized bed. Mass transfer was monitored using the *COD* parameter. It is shown that the operating conditions that give the best results are  $V_b/V_R = 0.55$  and a gas velocity of  $0.024 \text{ m s}^{-1}$ .

The inverse fluidized bed was used for the treatment of wastewater containing starch.<sup>4</sup> The experiments were performed in a column with a diameter of 9.2 mm and a height of 1.6 m. Irregularly shaped polypropylene particles with a density of  $870 \text{ kg m}^{-3}$  were used as carrier particles. Mass transfer was monitored using the *COD* parameter. The reduction of the *COD* parameter increased with the air flow rate and with the duration of the experiment. Wastewater treatment in an inverse fluidized system was investigated by Karmanev and Nikolov.<sup>5</sup> Spherical polystyrene particles with an average diameter of 2.5 mm and density of  $200 \text{ kg m}^{-3}$  were used as carriers. It can be seen that biochemical oxygen demand (*BOD*) decreases with time. It has been confirmed that inverse fluidization systems are an effective system for treating wastewater with low pollutant concentrations.

The knowledge of mass transfer is necessary for the application of inverse fluidized beds. One of the few papers dealing with the study of mass transfer in an inverse fluidized bed is the work of Nikov and Karamanev<sup>6</sup> who showed that better mass transfer is achieved by increasing the density difference between fluid and particles. The experimental data were compared with the literature correlations for mass transfer and the following correlation was proposed:

$$\text{Sh} = 0.28(\text{GaMvSc})^{0.33} \quad (1)$$

The experiments were carried out with polystyrene and polyethylene particles with a diameter of 2.2–7.1 mm and a density of 80–930 kg m<sup>-3</sup>. The fluidization medium was water and an aqueous solution of polyethylene glycol with a concentration of 1.9 % by mass. In their work, Kumar *et al.*<sup>7</sup> monitored mass transfer in an inverse fluidized system using electrochemical methods. Mass transfer of lead ions was monitored by an electrochemical method in an inverse fluidized bed, where the fluidization medium was an aqueous solution of ferrous salts and ferricyanide in the presence of sodium hydroxide. Cylindrical particles with a diameter of 2.151 mm and a height of 5 mm and a density of 877.6 kg m<sup>-3</sup> were used. The inverse fluidization was performed in a column with a diameter of 25.4 mm. As a result of these investigations, a correlation was established for the determination of the mass transfer factor:

$$j_D \varepsilon = 0.18 \left( \frac{\text{Re}_p}{1 - \varepsilon} \right)^{-0.30} \quad (2)$$

The aim of this work is to investigate wall-fluid mass transfer in the presence of inverse fluidized particles using the adsorption method. The experimental results are presented as a function of particle and bed parameters and compared with mass transfers in conventional fluidized beds.

#### EXPERIMENTAL

The scheme of the experimental apparatus is shown in Fig. 1. A cylindrical column with an inner diameter of 45 mm was used. At the top of the column there is a ring, on the inside of which there is a thin aluminium foil coated with silica gel. The column's inner diameter was not affected by the presence of the foil. The fluidization medium was a dilute aqueous solution of methylene blue with a concentration of  $2 \times 10^{-3}$  g L<sup>-1</sup>. The experiments were performed at a temperature of 20 °C. Spherical and non-spherical polypropylene and polyethylene particles were used for the experiments, and their properties are given in Table I.

During the fluid flow from the top of the column, an inverse fluidized bed was formed in which methylene blue adsorbed on silica gel during the experiment, *i.e.*, fluid-wall mass transfer occurred in the presence of inert particles. One of the conditions for the application of the method is a short adsorption time to avoid saturation of the adsorption surface, therefore the experiments lasted about 5 min.<sup>8-10</sup>

At the end of each experiment, the coloration of the surface of the silica gel foil, which is equivalent to the adsorbed amount of methylene blue, was analysed using SigmaScan Pro

software.<sup>10-12</sup> Based on the surface concentration, the mass transfer coefficient was determined according to the following equation:

$$k = \frac{c_p}{c_0 t} \quad (3)$$

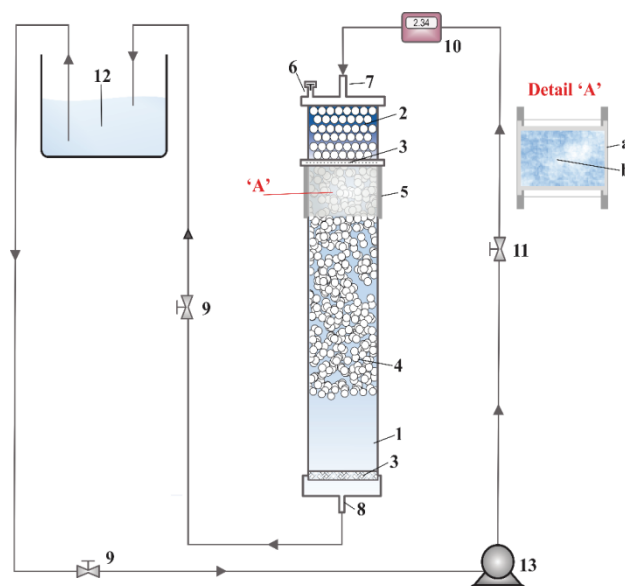


Fig. 1. Scheme of the experimental apparatus (1 – cylindrical column for inverse fluidization; 2 – distributor; 3 – grid; 4 – fluidized bed particles; 5 – inlet of the solution into the column; 6 – vent; 7 – piezometers; 8 – exit of the solution from the column; 9, 11 – valves; 10 – flow meter; 12 – reservoir; 13 – pump, 'A' – ring, a – silica gel foil, b – particles and methylene blue solution).

TABLE I. Properties of particles

Material	Diameter, mm	Sphericity	Density, kg m <sup>-3</sup>
Polypropylene	3.3	1	935
Polypropylene	3.7	0.86	935
Polypropylene	4.4	0.85	937
Polyethylene	3.9	0.87	926

## RESULTS AND DISCUSSION

Fig. 2 shows the dependence of the mass transfer coefficient (Eq. (3)) on the fluid velocity in the packed and in the inverse fluidized bed. The dependence shows a significant increase in the mass transfer coefficient at lower velocities, *i.e.*, in a packed bed of particles.

After reaching the fluidized state, the mass transfer coefficient increases slightly or is approximately constant. There are no significant differences in mass transfer in the bed with different particles because the differences in diameters

and sphericity are relatively small. For comparison, the mass transfer coefficient is also shown in the same diagram for a single-phase flow, *i.e.*, when only liquid (without particles) flows through the column. It can be seen that the presence of inert fluidized particles has no significant effect on mass transfer, probably due to the fact that the particle density is close to the liquid density.

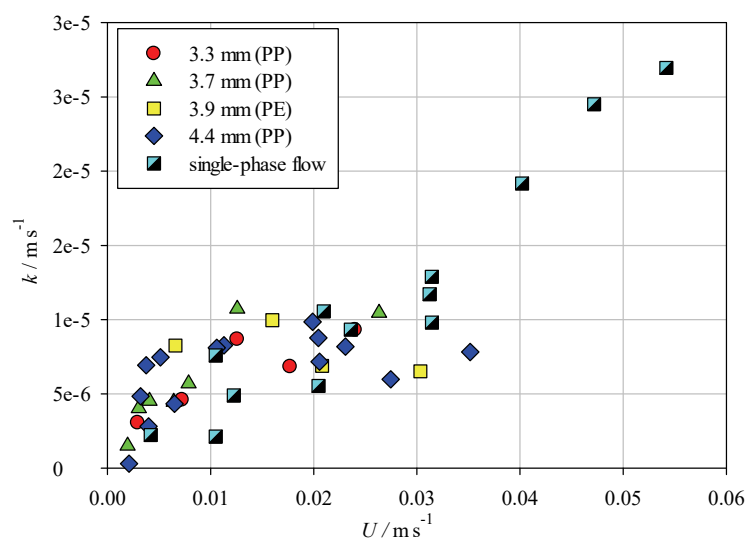


Fig. 2. Mass transfer coefficient in inverse fluidized bed and single-phase flow depending on fluid velocity.

A somewhat clearer dependence of the mass transfer coefficient on the bed parameters can be observed from the dependence of the Sherwood number ( $Sh$ ) on the Reynolds number ( $Re$ ), Fig. 3. From Fig. 3, it can be seen that the  $Sh$  in the fixed bed increases sharply with  $Re$  (*i.e.*, with the increase of the velocity  $U$ ). In the fluidized bed,  $Sh$  also increases with the increase in  $Re$ , but somewhat less than in the packed bed. It is also evident that there is no effect of particle size and shape on the mass transfer coefficient in the inverse fluidized bed, since all the particles studied show a very similar dependence.

Fig. 4 shows the dependence of the mass transfer coefficient on the bed porosity  $\varepsilon$ . Since the bed porosity is a function of  $U$ , the dependence of  $k = f(\varepsilon)$  practically follows the dependence of  $k = f(U)$ , Fig. 2. In a packed bed, where the porosity is constant, the mass transfer coefficient increases. During the transition to the fluidized bed state up to a bed porosity of about 0.7, the mass transfer coefficient continues to increase, while for higher values of bed porosity it becomes almost constant. Fig. 4 shows the appearance of a slight maximum on the curve, which also occurs with conventional fluidization.<sup>10</sup> It is also evident that there is

no visible difference in the intensity of mass transfer in the inverse fluidized bed with different particle types and sizes.

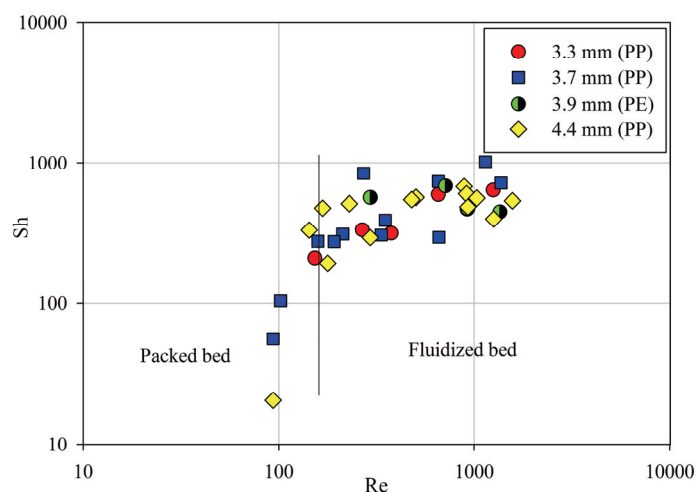


Fig. 3. Dependence of Sherwood on Reynolds number.

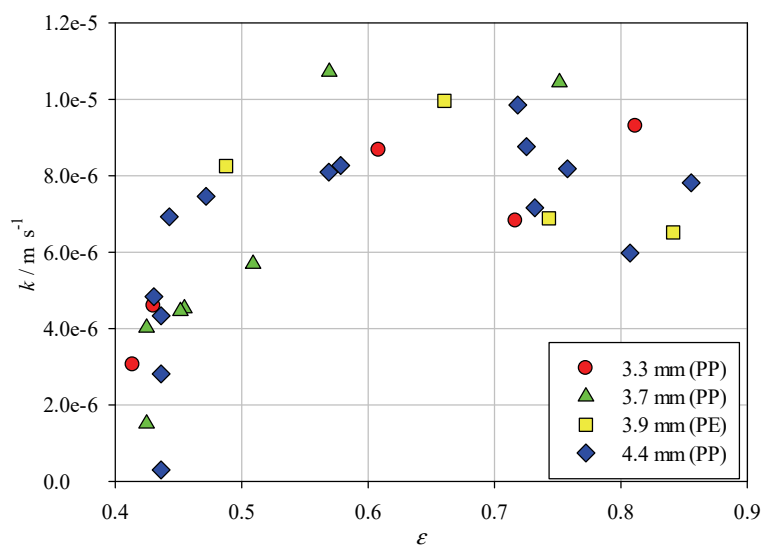


Fig. 4. Dependence of mass transfer coefficient on bed porosity for inverse fluidized bed (packed and fluidized bed).

The adsorption method used in this study to determine the mass transfer coefficient is also useful for flow visualization. Fig. 5 shows flow visualization images for different conditions (flows) of 4.4 mm diameter polypropylene particles in the bed. The chromatograms are shown for the same experimental con-

ditions (time duration, temperature, methylene blue concentration, *etc.*) but for different liquid flow rates. Fig. 5a–c are characteristic of the liquid flow where the particles are stable, *i.e.*, the packed bed. The flow patterns of the individual particles in the bed can be clearly seen. As the flow increases, it can be seen that the average colour intensity of the silica gel foil surfaces becomes higher. At the minimum fluidization velocity  $U_{mf}$  (Fig. 5d), the coloration of the silica gel foil surface is approximately uniform as the particles begin to oscillate slightly and mix the fluid. Fig. 5e and f are chromatograms taken in the fluidized bed and are characterized by the uniform coloration of the silica gel foil surface due to the intense mixing of the fluid by the particle fluidization. It can also be seen that the coloration of the surface is approximately the same at a higher flow rate in the fluidized bed.

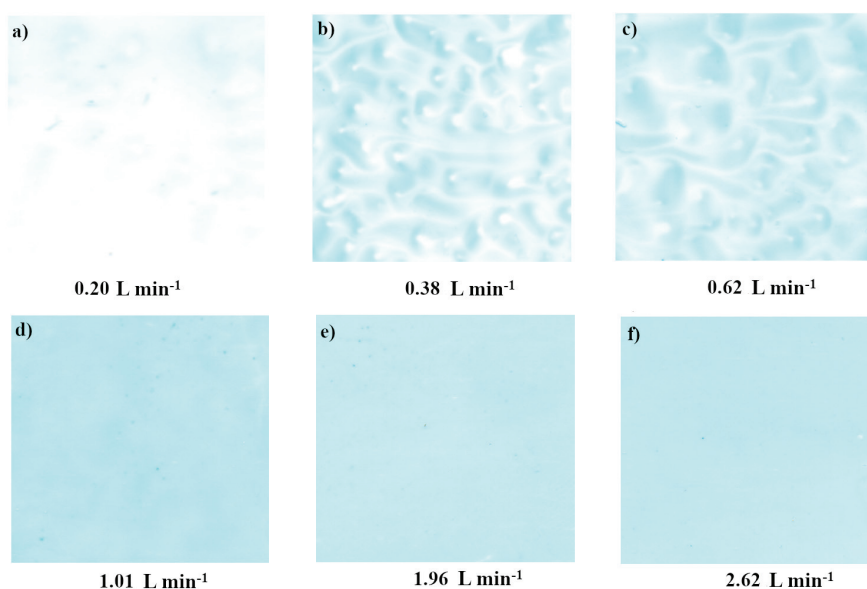


Fig. 5. Flow chromatogram in packed bed (a–c), at minimum fluidization (d) and in fluidized bed (e and f).

A comparison of the data obtained in inverse fluidized beds with those of a conventional fluidized bed as a function of bed porosity is shown in Fig. 6. The results presented for the conventional fluidized bed were carried out in a bed of spherical glass particles with a diameter of 3 mm and a density of  $2,500 \text{ kg m}^{-3}$  with water as the fluidizing medium. These experiments were carried out under the same experimental conditions and in the same column. From the dependencies shown in Fig. 6, it can be seen that the influence of the particles on mass transfer in conventional fluidization is significantly greater than the influence of

the particles in inverse fluidization. This can be explained by the fact that significantly higher fluid velocities were used in conventional fluidization compared to inverse fluidization. Fig. 6 shows the occurrence of a maximum at a porosity of about 0.7, which is consistent with our previous studies.<sup>9,13</sup>

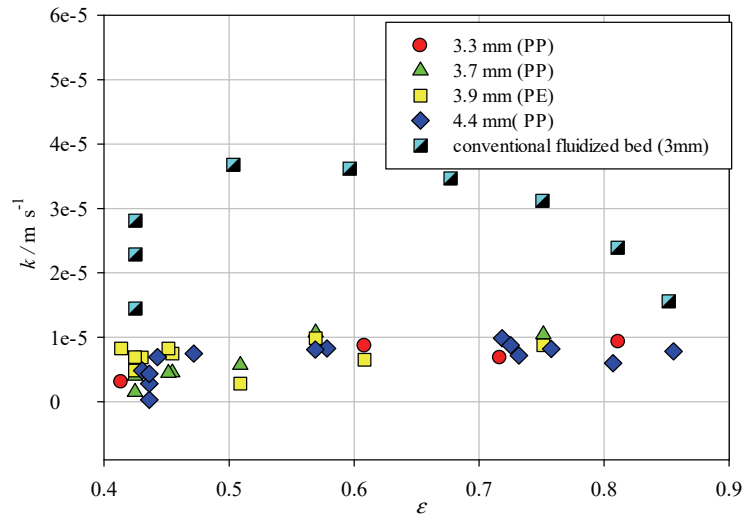


Fig. 6. Comparison of the mass transfer coefficient in inverse and conventional fluidized beds as a function of porosity.

Based on the experimentally determined results for the mass transfer coefficient, the mass transfer factor  $j_D$  was calculated. Fig. 7 shows the dependence of the mass transfer factor  $j_D$  on  $Re$  (Fig. 7a) and the porosity of the bed (Fig. 7b). Both dependences show a decrease in the mass transfer factor  $j_D$  with an increase in  $Re$  and the porosity of the bed which is consistent with our previous study.<sup>10</sup>

The diagram of the dependence of the mass transfer factor on  $Re$  also shows the data obtained for a single-phase fluid flow (Fig. 7a). It can be observed that the influence of the inverse fluidized particles on the mass transfer intensification is very small. This can be explained by the fact that in inverse fluidization the fluid velocity is low and therefore the collisions between the particles in the system are lower, so the influence on mass transfer is smaller.

The drag force in conventional fluidized beds is defined as:

$$F_d = F_b - F_g = \frac{d_p^3 \pi}{6} (\rho_p - \rho_f) g \quad (4)$$

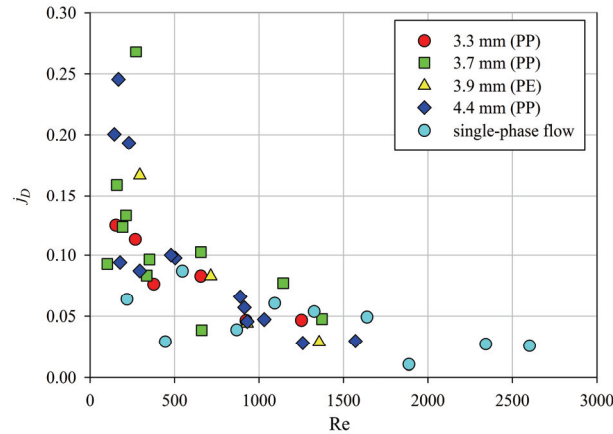
In inverse fluidized bed is defined as:

$$F_{d,inv} = F_g - F_b = \frac{d_p^3 \pi}{6} (\rho_f - \rho_p) g \quad (5)$$

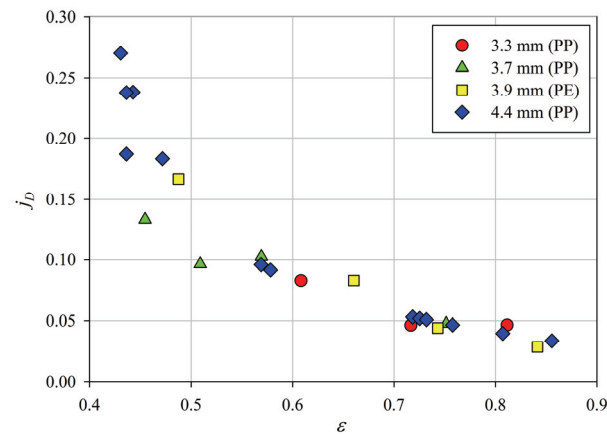


The ratio of the drag force in these two systems is:

$$\frac{F_d}{F_{d,inv}} = \frac{d_p^3}{d_{p,inv}^3} \frac{\rho_p - \rho_f}{\rho_f - \rho_p} \quad (6)$$



(a)



(b)

Fig. 7. Dependence of the mass transfer factor on Reynolds number (a) and bed porosity (b).

Comparing conventional fluidization, in which particles with a diameter of 3 mm and a density of  $2,500 \text{ kg m}^{-3}$  were used, with inverse fluidization, in which particles with a diameter of 3.7 mm and a density of  $935 \text{ kg m}^{-3}$  were used (the fluid density in both cases is  $1000 \text{ kg m}^{-3}$ ), the following relationship is obtained:

$$\frac{F_d}{F_{d,inv}} = 3.63 \quad (7)$$

It is found that the friction in the inverse fluidized bed is 3.6 times lower than in the conventional fluidized bed. Due to the small effect of particle–fluid friction in the inverse fluidized bed, the entire bed can be treated as a pseudo-fluid. All this indicates that although the conventional and inverse fluidized beds are described by the same equations, the frictional force is lower in the case of the inverse fluidized bed, so it is mainly used in biofilm reactors where the frictional forces do not disturb the formed biofilm, which is important for mass transfer in such reactors. The system behaves like a pseudo-fluid, and the frictional forces do not damage the biofilm. On the other hand, the particles are still present and provide gentle mixing, which is ideal for biosystems where microorganisms are involved in the reaction:<sup>14,15</sup>

$$\text{Re}_{\text{pf}} = \frac{d_p \rho_{\text{pf}} U_{\text{pf}}}{\mu_{\text{pf}}} \quad (8)$$

where pseudo-fluid density is defined as:

$$\rho_{\text{pf}} = \varepsilon \rho_f + (1 - \varepsilon) \rho_p \quad (9)$$

and pseudo-fluid dynamic viscosity as:

$$\mu_{\text{pf}} = \mu_f \exp\left(\frac{5(1 - \varepsilon)}{3\varepsilon}\right) \quad (10)$$

Superficial fluid velocity can be calculated:

$$U_{\text{pf}} = \frac{G_f}{\rho_f A} + \frac{G_p}{\rho_p A} \quad (11)$$

Since in a particulate fluidized bed the total particle motion in the column is zero ( $G_p = 0$ ), the velocity of the pseudo-fluid is equal to the superficial fluid velocity:

$$U_{\text{pf}} = \frac{G_f}{\rho_f A} = U \quad (12)$$

Based on the experimental results, the equation for the mass transfer factor was established:

$$j_D = \text{Re}_{\text{pf}}^{-0.48}, \quad 13 < \text{Re}_{\text{pf}} < 980 \quad (13)$$

Fig. 8 shows the dependence of the mass transfer factor  $j_D$  on the Reynolds number of a pseudo-fluid,  $\text{Re}_{\text{pf}}$ . The obtained equation agrees well with the experimental data. The mean absolute deviation of the experimental data from the data calculated by the established equation is 14.1 %, while the relative deviation is –4 %.

Table II shows some selected correlations for the determination of mass transfer factors in conventional and inverse fluidized beds and compares them

with our experimentally obtained data. The comparison of the experimental data with the data calculated according to the above correlations is shown in Fig. 9.

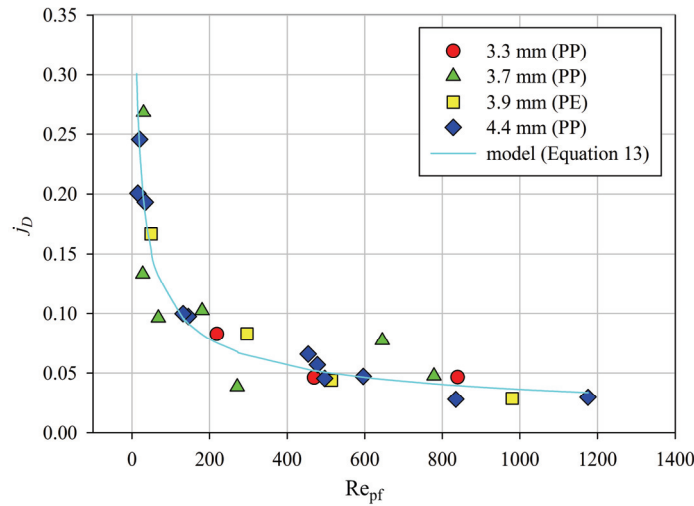


Fig. 8. Dependence of the mass transfer factor on the Reynolds number of a pseudo-fluid.

It is interesting to note that the correlation of Yutani *et al.*<sup>16</sup> (Eq. (14)), was originally derived for conventional fluidized beds, and the correlation of Nikov and Karamanev<sup>6</sup> (Eq. (17)) for inverse fluidized beds shows significant deviation from the experimental data. Very good agreement with the experimental data is shown by the correlations for conventional fluidization of Marooka *et al.*<sup>17</sup> (Eq. (15)) and Kunii and Levenspiel<sup>18</sup> (Eq. (16)), as can be seen in Table II.

TABLE II. Comparison of literature correlations with experimental data and the obtained model

Authors	Fluidization	Model	$\sigma_R, \%$	$\sigma_A, \%$
Yutani <i>et al.</i> <sup>16</sup> (Eq. (14))	Conventional	$j_D = \frac{0.4}{\varepsilon} Re_p^{0.4}$	71.5	73.5
Marooka <i>et al.</i> <sup>17</sup> (Eq. (15))	Conventional	$j_D = \frac{0.6}{\varepsilon} \left( \frac{Re_p}{1-\varepsilon} \right)^{-0.5}$	-6.93	14.9
Kunii and Levenspiel <sup>18</sup> (Eq. (16))	Conventional	$j_D = \frac{2}{Re_p} + \frac{0.51}{Re_p} [(1-\varepsilon)Re_p]^{-0.5}$	-0.89	14.6
Nikov and Karamanev <sup>6</sup> (Eq. (17))	Inverse	$j_D = \frac{0.28}{Re} (GaMv)^{0.33}$	-82.4	81.5
Our correlation (Eq. (13))	Inverse	$j_D = Re_{pf}^{-0.48}$	-4.0	14.1

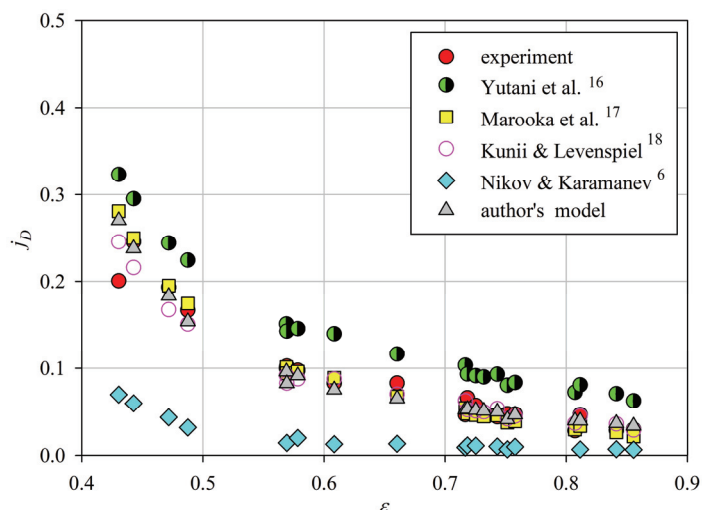


Fig. 9. Comparison of the experimental data with the obtained model and the correlations in the literature.

#### CONCLUSION

In the paper, the fluid–wall mass transfer coefficient was experimentally determined in an inverse fluidized bed. The results show a significant increase in the mass transfer coefficient with flow velocity in the packed bed, while a slight increase is observed in the fluidized bed. Compared to the mass transfers in a fluid flow without particles, it was found that the presence of particles does not contribute significantly to the intensification of the transfer, which is due to the low frictional force between particles and fluid. Based on the obtained results, the inverse fluidized bed was classified as a pseudofluid and a new correlation was presented, which represents the dependence of the mass transfer factor on the Reynolds number of a pseudo-fluid:

$$j_D = \text{Re}_{\text{pf}}^{-0.48}, \quad 13 < \text{Re}_{\text{pf}} < 980$$

The obtained experimental results deviate from the proposed correlation by less than 14.1 %, with the mean relative deviation being –4 %.

When comparing the experimentally obtained data with the correlations from the literature, it was found that the correlations of Marooka *et al.*<sup>17</sup> (Eq. (15)) and Kunii and Levenspiel<sup>18</sup> (Eq. (16)) for conventional fluidization show very good agreement with the experimental data.

#### NOMENCLATURE

<i>BOD</i>	biochemical oxygen demand
<i>COD</i>	chemical oxygen demand
<i>A</i>	cross section area, m <sup>2</sup>
<i>c<sub>p</sub></i>	surface concentration of methylene blue on adsorbent layer, kg m <sup>-2</sup>

$c_0$	bulk concentration of methylene blue, $\text{kg m}^{-2}$
$d_{p,\text{inv}}$	particle diameter in inverse fluidized bed, m
$d_p$	particle diameter, m
$D_c$	column diameter, m
$F_D$	drag force, N
$F_b$	buoyancy force, N
$F_g$	gravity force, N
$g$	gravitational acceleration, $\text{m s}^{-2}$
$G_f$	mass flow fluids, $\text{kg s}^{-1}$
$G_p$	mass flow particle, $\text{kg s}^{-1}$
$j_D$	mass transfer factor
$k$	coefficient mass transfer, $\text{m s}^{-1}$
$t$	time, s
$U$	superficial fluid velocity, $\text{m s}^{-1}$
$U_{\text{pf}}$	superficial pseudofluid velocity, $\text{m s}^{-1}$
$V_b/V_R$	ratio of the volume of the settled bed to the working volume
$\varepsilon$	bed porosity
$\mu_f$	viscosity fluid, $\text{Pa}\cdot\text{s}$
$\mu_{\text{pf}}$	viscosity pseudofluids, $\text{Pa}\cdot\text{s}$
$\rho_f$	fluid density, $\text{kg m}^{-3}$
$\rho_p$	particle density, $\text{kg m}^{-3}$
$\rho_{\text{pf}}$	pseudofluid density, $\text{kg m}^{-3}$
$Ga$	$(d_p^3 \rho_f^2 g / \mu_f^2)$ , Galileo number
$Mv$	$((\rho_p - \rho_f) / \rho_f)$ , relative density
$Re$	$(U_f D_c \rho_f / \mu_f)$ , Reynolds number
$Re_p$	$(U_f d_p \rho_f / \mu_f)$ , Reynolds number for particle
$Re_{\text{pf}}$	Reynolds number for pseudo-fluid
$Sh$	$(k D_c / D_{AB})$ , Sherwood number
$Sc$	$(\mu_f / \rho_f D_{AB})$ , Schmidt number
$\sigma_A$	$\left( \frac{1}{N} \sum_1^N \left  \frac{X_{\text{exp}} - X_{\text{cal}}}{X_{\text{exp}}} \right  \right)$ , absolute deviations
$\sigma_R$	$\left( \frac{1}{N} \sum_1^N \frac{X_{\text{exp}} - X_{\text{cal}}}{X_{\text{exp}}} \right)$ , relative deviations

*Acknowledgement.* This work was financially supported by the Ministry of Science, Technological Development and Innovation of the Republic of Serbia (Grant No. 451-03-47/2023-01/200026 and 451-03-47/2023- 01/200135).

## ИЗВОД

## ПРЕНОС МАСЕ У ИНВЕРЗНО-ФЛУИДИЗОВАНОМ СЛОЈУ

ДАРКО ЈАЃИМОВСКИ<sup>1</sup>, КАТАРИНА ШУЋУРОВИЋ<sup>1</sup>, МИХАЛ ЂУРИШ<sup>1</sup>, ЗОРАНА АРСЕНИЈЕВИЋ<sup>1</sup>, САЊА КРСТИЋ<sup>2</sup> и НЕВЕНКА БОШКОВИЋ-ВРАГОЛОВИЋ<sup>3</sup>

<sup>1</sup>Институт за хемију, технологију и металургију-Институт од националне значаја за Републику Србију, Универзитет у Београду, Београд, <sup>2</sup>Винча Институт за нуклеарне науке-Институт од националне значаја за Републику Србију, Универзитет у Београду, Београд и <sup>3</sup>Технолошко-металуршки факултет, Универзитет у Београду, Београд

У овом раду је одређиван коефицијент преноса масе флуид-зид у инверзно-флуидизованом слоју применом адсорпционе методе. Експерименти су вршени у колони пречника 45 mm са сферичним и несферичним честицама полипропилена и полиетиленом пречника 3,3–4,9 mm и густине око 930 kg m<sup>-3</sup>. Као флуидизациони медијум коришћен је разблажени раствор метиленског плавог који је адсорбован на делу површине колоне на силикагелу. Добијени резултати показали су да присуство честица при инверзној флуидизацији не доприноси значајно преносу масе у поређењу са утицајем честица на пренос масе у конвенционално флуидизованим слојевима. Због тога је у анализу уведен концепт псеудофлуида и изведена је емпиријска корелација за одређивање коефицијента преноса масе. Извршено је поређење добијених резултата са литературним корелацијама за инверзну и конвенционалну флуидизације.

(Примљено 16. јануара, ревидирано 27. фебруара, прихваћено 22. марта 2023)

## REFERENCES

1. D. Wang, T. Silbaugh, R. Pfeffer Y. S. Lin, *Powder Technol.* **203** (2010) 298 (<https://doi.org/10.1016/j.powtec.2010.05.021>)
2. S. S. Begum, K. V. Radha, *Korean J. Chem. Eng.* **31** (2014) 436 (<https://doi.org/10.1007/s11814-013-0260-z>)
3. W. Sokol, A. Ambaw, B. Woldeyes, *Chem. Eng. J.* **150** (2009) 63 (<https://doi.org/10.1016/j.cej.2008.12.021>)
4. M. Rajasimman, C. Karthikeyan, *Int. J. Environ. Res.* **3** (2009) 569 (<https://doi.org/10.22059/IJER.2010.72>)
5. D.G. Karamanov, L.N. Nikolov, *Environ. Prog.* **15** (1996) 3 (<https://doi.org/10.1002/ep.670150319>)
6. I. Nikov, D. Karamanov, *AIChE J.* **37** (1991) 781 (<https://doi.org/10.1002/aic.690370515>)
7. K.A. Kumar, G.V.S. Sarma, M. Vijay, K.V. Ramesh, *Test Eng. Manage.* **83** (2020) 14318 (<http://www.testmagazine.biz/index.php/testmagazine/article/view/9657/7397>)
8. S. Končar-Durđević, *Nature* **172**, 878 (1953) 858 (<https://doi.org/10.1134/S0036024409090246>)
9. D. Jaćimovski, *PhD Thesis*, Faculty of Technology and Metallurgy, Belgrade, 2017 (<http://phaidrabbg.bg.ac.rs/o:17299>)
10. N. Bošković-Vragolović, R. Garić-Grulović, Ž. Grbavčić, R. Pjanović, *Russ. J. Phys. Chem.* **83** (2009) 1550 (<https://doi.org/10.1134/S0036024409090246>)
11. *SigmaScan Software*, Jandel Scientific, Erkrath, 1999
12. M. Đuriš, T. Kaluđerović Radoičić, R. Garić-Grulović, Z. Arsenijević, Ž. Grbavčić, *Powder Technol.* **246** (2013) 98 (<https://doi.org/10.1016/j.powtec.2013.05.009>)
13. D. Jaćimovski, R. Garić-Grulović, N. Vučetić, R. Pjanović, N. Bošković-Vragolović, *Powder Technol.* **303** (2016) 68 (<https://doi.org/10.1016/J.powtec.2016.09.025>)

14. Ž.Grbavčić, Z. Arsenijević, R.Garić-Grulović, *Powder Technol.* **190** (2009) 283  
(<https://doi.org/10.1016/j.powtec.2008.08.005>)
15. R. Garić-Grulović, Ž. Grbavčić, Z. Arsenijević, *J. Serb. Chem. Soc.* **70** (2005) 775  
(<http://dx.doi.org/10.2298/JSC0505775G>)
16. N. Yutani, N. Ototake, L.T. Fan, *Ind. Eng. Chem. Res.* **26** (1987) 343  
(<https://doi.org/10.1021/ie00062a028>)
17. S. Marooka, K. Kusakabe, Y. Kato, *Int. Chem. Eng.* **20** (1980) 433
18. D. Kunii, O. Levenspiel, *Fluidisation Engineering*, Wiley, New York, 1969, p. 195.